

Doped graphene: the interplay between localization and frustration due to the underlying triangular symmetry

This article has been downloaded from IOPscience. Please scroll down to see the full text article.

2011 J. Phys.: Condens. Matter 23 375501

(<http://iopscience.iop.org/0953-8984/23/37/375501>)

View [the table of contents for this issue](#), or go to the [journal homepage](#) for more

Download details:

IP Address: 132.248.7.39

The article was downloaded on 01/09/2011 at 16:29

Please note that [terms and conditions apply](#).

Doped graphene: the interplay between localization and frustration due to the underlying triangular symmetry

J E Barrios-Vargas and Gerardo G Naumis

Departamento de Física-Química, Instituto de Física, Universidad Nacional Autónoma de México (UNAM), Apartado Postal 20-364, 01000, México DF, México

E-mail: naumis@fisica.unam.mx

Received 13 June 2011, in final form 5 August 2011

Published 31 August 2011

Online at stacks.iop.org/JPhysCM/23/375501

Abstract

An intuitive explanation of the increase in localization observed near the Dirac point in doped graphene is presented. To do this, we renormalize the tight binding Hamiltonians in such a way that the honeycomb lattice maps into a triangular one. Then, we investigate the frustration effects that emerge in this Hamiltonian. In this doped triangular lattice, the eigenstates have a bonding and antibonding contribution near the Dirac point, and thus there is a kind of Lifshitz tail. The increase in frustration is related to an increase in localization, since the number of frustrated bonds decreases with disorder, while the frustration contribution raises.

(Some figures in this article are in colour only in the electronic version)

Since its discovery [1], graphene has become *ipso facto* a viable material for designing nanoelectronic devices due to its unusual transport properties [2–4]. At room temperature, graphene has a high electrical [5] and thermal conductivity [6]. However, the electrical conductivity is difficult to manipulate by means of an external gate voltage [7, 8], a situation that turns out to be a problem in the construction of field effect transistors. This is due to the fact that graphene does not have a gap, i.e. it is a semi-metallic material. An alternative is to induce localized states by adding non-carbon atom impurities to the lattice. This method has been proved theoretically [9, 10] and experimentally [11, 12]. This leads to the appearance of resonant or localized states around the Dirac point, with two energies that separates states with different degrees of localization [9, 13], i.e. the states near the Dirac point are much more localized than the rest of the states in the band. It is worthwhile mentioning that such energies are similar to mobility edges; however, in doped graphene all states are localized [14–16] except at the Dirac point [17], in agreement with the usual picture of Anderson localization. Thus, we will refer to such energies separating states with very different localization degrees as pseudo-mobility edges.

A recent scaling analysis of the inverse participation ratio [18] has confirmed the existence of these pseudo-

mobility edges seen by [9]. In [9], we used a variational method to prove the fundamental role of frustration of the electronic wave function in such a process. In this paper, we revisit the problem by evaluating numerically the ideas behind the proposed scenario, i.e. we map the honeycomb graphene lattice into a triangular one, just by removing one of the bipartite sublattices. This process is equivalent to taking the squared Hamiltonian. Then a frustration effect appears near the antibonding limit, which corresponds exactly to the Dirac point. This explains why there is increased localization, since defects enhance frustration producing a kind of Lifshitz tail [19]. We consider the phase between neighboring sites in the underlying triangular lattice, since in the renormalized graphene lattice there is competition between antibonding and bonding bonds. Also, the pseudo-mobility edges near the Dirac point are the simple result of unfolding the mobility edge that appears at the squared Hamiltonian. The general background of the renormalized Hamiltonian is included in the following paragraphs, as well as the results and discussion.

As a model, consider pure graphene with substitutional non-carbon atoms distributed randomly on the lattice. We model this system by using a tight binding Hamiltonian approximation:

$$H = H_C + H_I, \quad (1)$$

where H_C is the usual nearest-neighbor Hamiltonian of pure graphene. Using the fact that the lattice can be separated into two interpenetrating triangular sublattices [20], A and B , the Hamiltonian is given by

$$H_C = -t \sum_i |A_i\rangle\langle B_i| + |B_i\rangle\langle A_i|, \quad (2)$$

where $t \approx 2.79$ eV is the nearest-neighbor hopping energy,

$$H_I = \varepsilon \sum_l |l\rangle\langle l| \quad (3)$$

is the Hamiltonian due to impurities (ε is the energy difference between a carbon atom and a foreign atom) and $|l\rangle = |A_l\rangle$ or $|B_l\rangle$. The impurities are randomly distributed along the lattice with concentration x .

In the limit $\varepsilon \gg t$ the bands are separated, and we can suppose that the wave functions on the carbon band do not have amplitude in the impurity sites and vice versa, although corrections are easily obtained by using a power series [21] on t/ε . Impurities are thus considered as holes in the pure graphene lattice, and the bipartite character is preserved. This allows us to renormalize the lattice using the squared Hamiltonian [9], H^2 . By looking at the eigenvalues E^2 of H^2 , this method leads us to separate the contributions for a given energy as [22, 9]

$$E^2 = \sum_i Z_i t^2 |c_i(E)|^2 + \sum_{j \neq i} (H_C^2)_{ij} c_j(E) c_i^*(E), \quad (4)$$

where $c_i(E)$ is the amplitude of the wave function at site i for an eigenenergy E . Here, sites i and j are no longer in a honeycomb lattice; they belong to a triangular lattice which results from a deletion of one of the bipartite lattices (see figure 1). Notice that in (4), Z_i is the coordination of site i in the original lattice with Hamiltonian H . The spectrum of H^2 is basically obtained by folding the spectrum of H around 0. So, the states near the Dirac point, $E = 0$, become closer to antibonding states in a triangular lattice, as shown in figure 1 where we plot the density of states (DOS) of the honeycomb lattice $\rho(E)$ and triangular lattice $\rho(E^2)$. It is well known that such states are frustrated in a triangular lattice. If disorder is present this can lead to localization, since the wave function tends to avoid regions of high frustration, producing a kind of Lifshitz tail [19]. Thus, we can expect interesting effects since the Dirac point corresponds to the antibonding limit in a triangular lattice. Now let us examine such a scenario in more detail.

Equation (4) contains two contributions: one is the self-energy term, the other is the contribution in energy of each bond. Clearly, each bond can raise or decrease the energy depending on the sign of $c_j(E)c_i^*(E)$. From (4), we define

$$E^2 = C_1(E^2) - C_2(E^2) + C_3(E^2), \quad (5)$$

where $C_1(E^2) = \sum_i Z_i t^2 |c_i(E)|^2$ is the contribution of the self-energies, which depends on the Z_i of the original lattice. $C_2(E^2) = \sum_{j \neq i} (H_C^2)_{ij} |c_j(E)c_i^*(E)|$, where the prime means that one considers only those bonds whose product $c_j(E)c_i^*(E)$ is negative. This is the antibonding contribution. Finally, $C_3(E^2)$ is similar to $C_2(E^2)$, except that the summation is over

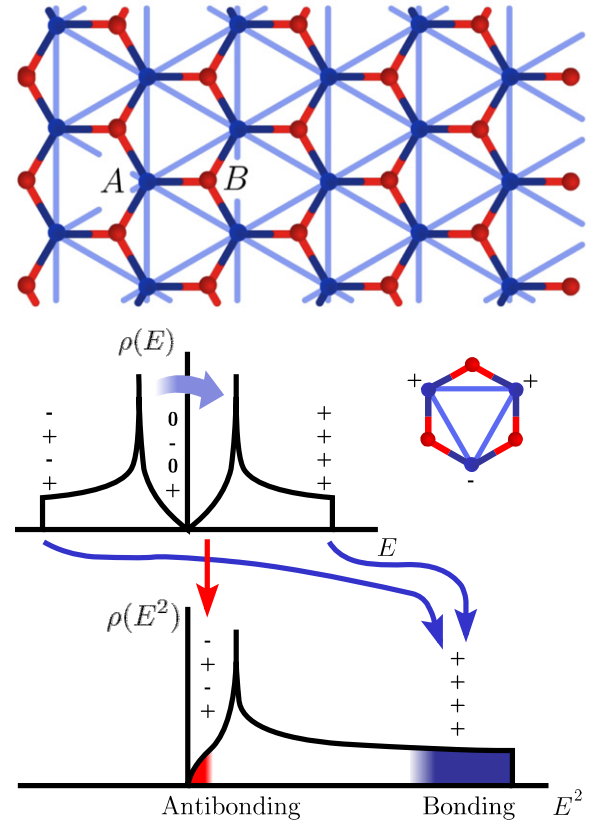


Figure 1. Schematic diagram of the map that transforms a hexagonal lattice into a triangular one. This is equivalent to folding the spectrum of the graphene Hamiltonian, H , into the one of H^2 , as seen in the DOS for each Hamiltonian. States near the Dirac point become frustrated antibonding states on a triangular lattice. The \pm signs, and zeros at each location in the spectrum represent schematic phase changes between neighbors. The central state in H is mapped into an antibonding state once the zeros are removed in one of the sublattices.

bonds with positive $c_j(E)c_i^*(E)$. To obtain a minimal energy for a state, $-C_2(E^2) + C_3(E^2)$ needs to be as low as possible since $C_1(E^2) > 0$.

For pure graphene, the contribution of each coefficient is shown in figure 2. As the coordination is $Z_i = 3$ for every site, and all $|c_i(E)|$ are equal, then $C_1(E^2)$ is a line at 3, as seen in figure 2. There is a considerable variation of the contributions $C_2(E^2)$ and $C_3(E^2)$ as function of E^2 ; this is a result of the degeneration in the spectrum. Thus, the graph shows an envelope for C_2 and C_3 ; in particular there is a maximal variation at the Van Hove singularity located at $(E/t)^2 = 1$. However, one clearly sees how the maximal E^2 , corresponding to $9t$, is obtained by making all bonds frustrated. As the energy is decreased, $C_3(E^2)$ goes down and $C_2(E^2)$ increases. The interesting region for conductivity is around the Fermi energy, $E^2 = 0$, where there is a frustration effect, i.e. there is a bonding and antibonding contribution to the energy. The corresponding C_2 and C_3 values are $(3/2\pi)(2\sqrt{3} + 4\pi/3) \approx 3.65$ and $(3/2\pi)(2\sqrt{3} - 2\pi/3) \approx 0.65$, obtained simply by looking at the phase differences of the minimal energy wave function on a triangular lattice.

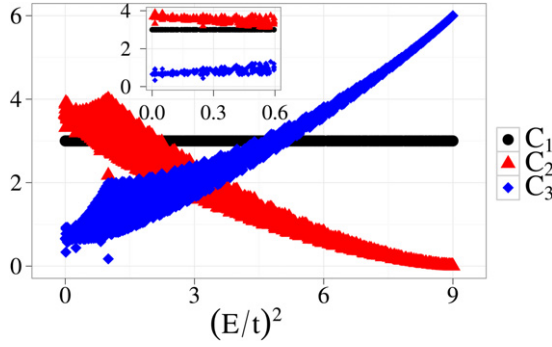


Figure 2. Energy contributions $C_1(E^2)$ (self-energy), $C_2(E^2)$ (antibonding) and $C_3(E^2)$ (bonding) for pure graphene, (5). The width in $C_2(E^2)$ and $C_3(E^2)$ is due to the degeneration of the spectrum, which is maximal at the Van Hove singularity ($E = 1$). Inset: amplification near the Dirac point. These results were obtained from a diagonalization of H for lattices of $N = 7688$ sites.

These numbers are in excellent agreement with the numerical simulations observed in the inset in figure 2. Such results were obtained by a direct diagonalization of the operator H for a lattice of $N = 7688$ sites, and confirm the hypothesis of the existence of antibonding states around the Dirac point.

Now we introduce the impurities in H . From a direct diagonalization of the operator H , we obtain figure 3 for $N = 7688$ sites. The behavior of $C_1(E^2)$ suggests an amplitude reduction in carbon sites around impurity sites near $E \approx 0$ as the doping x increases, since if we write the coordination and the amplitude as an average part plus fluctuation, $Z_i \equiv \langle Z \rangle + \delta Z_i$ and $|c_i(E)|^2 \equiv \langle |c(E)|^2 \rangle + \delta |c_i(E)|^2$, it is easy to show that

$$C_1(E^2) = 3(1-x) + \sum_{j \neq i} \delta Z_j \delta |c_j(E)|^2 \quad (6)$$

where we used that $\langle Z \rangle = 3(1-x)$, as obtained from a binomial distribution [9]. The first term in (6) is in perfect agreement for the highest energy, corresponding to the pure bonding state. However, the last term in (6) is the correlation between amplitude–coordination fluctuations. According to figure 3, $\delta Z_i \delta |c_i(E)|^2 < 0$ and grows in magnitude as $E^2 \rightarrow 0$. Thus, there is an anticorrelation, and the amplitude tends to grow in sites of lower coordination, i.e. around impurity sites.

Also from figure 3, we see that the spacings between $C_2(E^2)$ for different impurity concentrations x are always bigger than the ones corresponding to $C_3(E^2)$. Thus, figure 3 proves that there is an increase in the frustration term with x . There are some points in figure 3 that go to zero value; those points correspond to resonant states at impurities.

One of the interesting questions here is why $C_2(E^2)$ and $C_3(E^2)$ change in a different fashion. Is it due to an increased number of frustrated bonds or is it a consequence of amplitude changes in such bonds? In order to compare these variations for $C_2(E^2)$ and $C_3(E^2)$, we introduce the average contribution per bond

$$A_2 = \frac{C_2(E^2)}{N_A/N_T}, \quad A_3 = \frac{C_3(E^2)}{N_B/N_T}, \quad (7)$$

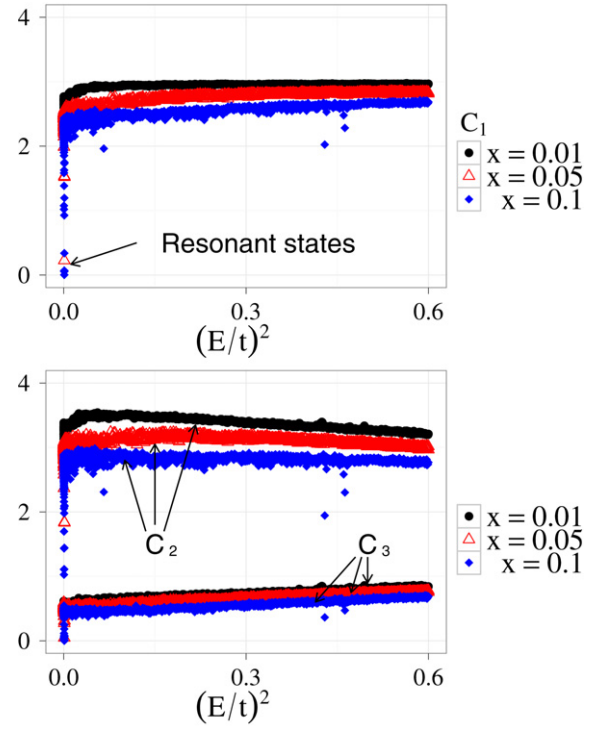


Figure 3. Energy contributions $C_1(E^2)$ (self-energy), $C_2(E^2)$ (antibonding) and $C_3(E^2)$ (bonding) for doped graphene. The reduction of $C_2(E^2)$ as x grows means that the antibonding contribution goes down, and thus frustration is increased. A drop near $E^2 \approx 0$ is also observed, corresponding to resonant states. These results were obtained from a diagonalization of H for lattices of $N = 7688$ sites.

where N_A is the total number of bonds where $c_j(E)c_i^*(E) < 0$, N_B corresponds to bonds where $c_j(E)c_i^*(E) > 0$, and N_T is the total number of bonds without considering links to impurity sites.

In this measurement scale it is evident that the antibonding contribution has a wider variation when compared with the bonding contribution as x grows (figure 4). Also, in figure 4 we present N_A as a function of E^2 . Since $N_B = N_T - N_A$, is clear that disorder increases N_A with respect to N_B . However, the average amplitude on each antibonding link is decreased with disorder, leading to higher frustration. This is a consequence of the inequality $C_1(E^2) + C_3(E^2) \geq C_2(E^2)$ obtained from (7) since $C_1(E^2)$ decreases as $(1-x)$ and $C_3(E^2)$ has only small changes. Thus, $C_2(E^2)$ must decrease accordingly and the pseudo-mobility edge seems to appear as a consequence of avoiding sites of high coordination which leads to high frustration. When the spectrum of H^2 is unfolded by taking the square root of E^2 , this edge is transformed in two edges, as shown using the inverse participation ratio calculated in [9].

In conclusion, the problem of graphene with impurities is mapped into a triangular lattice with holes. As a result, the Dirac point turns out to be an antibonding edge, where frustration effects are important due to the underlying triangular symmetry.

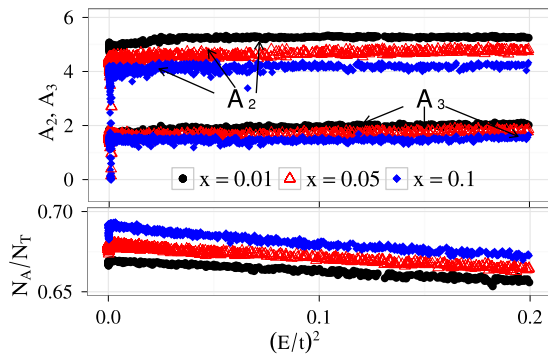


Figure 4. Top: average antibonding (A_2) and bonding contribution (A_3) per bond as a function of E^2 near $E^2 = 0$ for different concentrations x , as defined in (7). Notice how the antibonding contribution diminishes more than the bonding contribution with x , and thus the frustration per bond is increased. Bottom: total number of antibonding bonds, N_A , as a function of E^2 for different concentrations x . Since N_A increases and A_2 decreases for $E^2 \rightarrow 0$ and $x \rightarrow 1$, frustration is rising due to localization effects.

Acknowledgments

We thank the DGAPA-UNAM project IN-1003310-3. JEB-V acknowledges a scholarship from CONACyT (Mexico). Calculations were performed on Kanbalam supercomputers at DGSCA-UNAM.

References

- [1] Novoselov K S, Geim A K, Morozov S V, Jiang D, Zhang Y, Dubonos S V, Grigorieva I V and Firsov A A 2004 *Science* **306** 666–9
- [2] Geim A K and Novoselov K S 2007 *Nature Mater.* **6** 191
- [3] Peres N M R, Rodrigues J N B, Stauber T and Lopes dos Santos J M B 2009 *J. Phys.: Condens. Matter* **21** 344202
- [4] Geim A K 2009 *Science* **324** 1530–4
- [5] Novoselov K S, Geim A K, Morozov S V, Jiang D, Katsnelson M I, Grigorieva I V, Dubonos S V and Firsov A A 2005 *Nature* **438** 197–200
- [6] Balandin A A, Ghosh S, Bao W, Calizo I, Teweldebrhan D, Miao F and Lau C N 2008 *Nano Lett.* **8** 902–7
- [7] Avouris P, Chen Z and Perebeinos V 2007 *Nature Nanotechnol.* **2** 605–15
- [8] Xia F, Farmer D B, Lin Y and Avouris P 2010 *Nano Lett.* **10** 715–8
- [9] Naumis G G 2007 *Phys. Rev. B* **76** 153403
- [10] Martinazzo R, Casolo S and Tantardini G F 2010 *Phys. Rev. B* **81** 245420
- [11] Bostwick A, McChesney J L, Emtsev K V, Seyller T, Horn K, Kevan S D and Rotenberg E 2009 *Phys. Rev. Lett.* **103** 056404
- [12] Bostwick A, Ohta T, McChesney J L, Emtsev K V, Speck F, Seyller T, Horn K, Kevan S D and Rotenberg E 2010 *New J. Phys.* **12** 125014
- [13] Amini M, Jafari S A and Shahbazi F 2009 *Europhys. Lett.* **87** 37002
- [14] Aleiner I L and Efetov K B 2006 *Phys. Rev. Lett.* **97** 236801
- [15] Altland A 2006 *Phys. Rev. Lett.* **97** 236802
- [16] Ostrovsky P M, Gornyi I V and Mirlin A D 2006 *Phys. Rev. B* **74** 235443
- [17] Ostrovsky P M, Titov M, Bera S, Gornyi I V and Mirlin A D 2010 *Phys. Rev. Lett.* **105** 266803
- [18] Song Y, Song H and Feng S 2011 *J. Phys.: Condens. Matter* **23** 205501
- [19] Cohen M 1983 *Topological Disorder in Condensed Matter (Springer Series in Solid State Sciences vol 46)* ed F Yonezawa and T Ninomiya (New York: Springer) p 122
- [20] Castro Neto A H, Guinea F, Peres N M R, Novoselov K S and Geim A K 2009 *Rev. Mod. Phys.* **81** 109–62
- [21] Kirkpatrick S and Eggarter T P 1972 *Phys. Rev. B* **6** 3598–609
- [22] Naumis G G, Wang C and Barrio R A 2002 *Phys. Rev. B* **65** 134203